# Work function dependent neutralization of low-energy noble gas ions

R. Cortenraad,[1] A. W. Denier van der Gon,[1] H. H. Brongersma,[1,*] S. N. Ermolov,[2] and V. G. Glebovsky[2]
[1]*Eindhoven University of Technology, P.O. Box 513, 5600 MB Eindhoven, The Netherlands*
[2]*Institute of Solid State Physics, Chernogolovka Moscow distr., 142432 Russia*
(Received 31 October 2001; published 29 April 2002)

The work function dependence of the neutralization of low-energy $He^+$, $Ne^+$, and $Ar^+$ ions was studied by determining the neutralization probability of ions scattered from submonolayer coverages of Ba on W(110) and Re(0001) substrates. At high work functions (>3.5 eV), it was found that the dominant neutralization mechanism for noble gas ions with initial energy between 2 and 5 keV scattering from Ba is collision-induced neutralization. The neutralization probability for this mechanism was found to be insensitive to work function changes. We argue that collision-induced neutralization is also the dominant charge transfer process for scattering from other earth-alkali and alkali elements in this energy range, although at lower energies it is expected that Auger neutralization will become important. At work functions below roughly 3.5 eV, resonant neutralization to the first excited level of the noble gas ions occurs in addition to the charge transfer processes operating at high work functions. We show that the additional neutralization at low work functions can be described using resonant charge exchange theory. Due to resonant neutralization, the neutralization probability for noble gas ions increases exponentially with decreasing work function.

DOI: 10.1103/PhysRevB.65.195414 PACS number(s): 61.18.Bn; 34.50.Dy

## I. INTRODUCTION

Low-energy ion scattering (LEIS) using noble gas ions is a surface analysis technique that only probes the outermost atomic layer of the surface. This extreme surface sensitivity is the result of the high neutralization probability of noble gas ions during interaction with the surface atoms. Although LEIS is widely applied for investigations of the outermost atomic layer of many different types of solid surfaces, the neutralization mechanisms of noble gas ions have not yet been indisputably established and are still the subject of many investigations.

The subject of this paper is the work function dependence of the neutralization of noble gas ions. The neutralization mechanisms at low work functions are especially interesting because LEIS studies have shown a strong influence of the work function on the neutralization probability.[1–7] Several authors have suggested that at low work functions noble gas ions can be neutralized by a mechanism involving a (resonant) charge transfer to the first excited level of the ion.[2,4,8] However, a systematic investigation of the work function dependence of the neutralization probability at low work functions is absent in the literature.

We have investigated the neutralization behavior of $He^+$, $Ne^+$, and $Ar^+$ noble gas ions over a work function range extending from 6 eV down to 2 eV. The work function variation for these investigations was induced by adsorbing Ba on W(110) and Re(0001) single crystals. The neutralization probability for noble gas ions scattered from these systems was determined using the characteristic velocity method.[5,9,10] From the observed work function dependence of the neutralization, combined with results from neutralization studies reported in the literature, the nature of the neutralization mechanisms is deduced. In Sec. II a short overview of the possible neutralization mechanism for noble gas ions is given. For clarity, in this overview we have already incorporated to some extent the conclusions from our investigations. In the following sections of this paper we present the evidence for these conclusions. The experiments and the methods used to vary the work function are described in Sec. III. Subsequently, in Sec. IV we present and discuss the results of our investigations. The main conclusions are summarized in Sec. V.

## II. NEUTRALIZATION MECHANISMS

In LEIS, noble gas ions are directed onto the surface and the ions that scatter back from the surface are analyzed. Due to the interactions with the surface atoms, ions can be neutralized by several neutralization mechanisms: Auger neutralization (AN), collision-induced neutralization (CIN), and resonant neutralization (RN). The acronyms AN, CIN, and RN will be used throughout the remainder of the paper to indicate the respective neutralization mechanisms. Along the ion trajectory each of these mechanisms can occur at a specific interaction distance, which is different for the various mechanisms. Neutralization along the trajectory can be divided into three sections:[11,12] (1) the incoming trajectory, (2) the violent collision, and (3) the outgoing trajectory. Which mechanism(s) takes place depends on the ion-target combination, on the work function of the system, and on the energy of the ion. Several mechanisms may be operating simultaneously.

### A. Auger neutralization

In AN, an electron is transferred from the metal conduction band of the surface to the ground state of the ion.[13,14] The energy surplus of this transition is used to emit a second electron from the conduction band (see Fig. 1). Auger neutralization can take place when there is sufficient overlap between the orbitals of the ion and the surface atoms, which is the case at a distance of approximately 1–2 Å.[8,15] The neutralization probability depends on the density of electrons

 

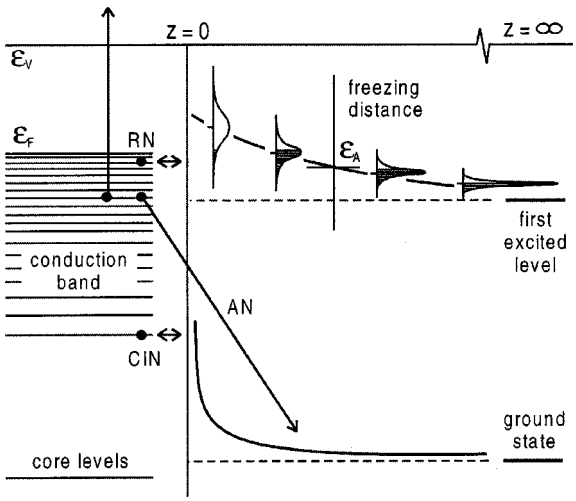


FIG. 1. Schematic representation of the different neutralization mechanisms. RN: resonant neutralization. AN: Auger neutralization. CIN: collision-induced neutralization.

available for the transition and is in first-order approximation proportional to the square of the electron density of the target atoms since two electrons are involved in the process.[16] The transition probability thus depends on the ion-target combination. Furthermore, the neutralization probability depends on the velocity of the ion: a slow ion spends more time within the spatial region where Auger transitions can take place and therefore has a large neutralization probability.

Since the pioneering work by Hagstrum,[13,14] AN is often assumed to be the dominant neutralization mechanism for noble gas ions due to the large ionization potentials of the ground state of the ions (see Table I). However, in this paper we show that the Auger process plays no significant role in the neutralization of noble gas ions scattered from alkali and alkali-earth elements, with an initial energy between 2 and 5 keV. Note that here we only consider small impact parameters that are required for ions to be backscattered (the impact parameter ranges between 0.02 and 0.09 Å in these studies, the distance of closest approach between 0.1 and 0.5 Å). At large impact parameters occurring for lower energies or smaller scattering angles, AN is expected to play an important role.

### B. Collision-induced neutralization

Several experimental and theoretical investigations have questioned the assumed dominance of the Auger mechanism and suggested that noble gas ions can also be neutralized during the violent collision between the ion and target atom.[11,12,17–19] Much work on this subject was performed by Boers[12] and later by Souda *et al.*[17] For the neutralization process at close encounter we will use the term CIN (collision-induced neutralization), as introduced by Souda *et al.*[17]

During the violent collision between ion and target atom, the ground state of the ion can be promoted due to its interaction with the core levels of the target atom.[20–22] At small distances, of the order of 0.5 Å, the ground state of the ion is aligned with the bottom of the conduction band, enabling resonant charge exchange between the ground state and the levels at the bottom of the band (see Fig. 1). Consequently, the noble gas ions can be neutralized, and ions that were neutralized on the incoming trajectory can be re-ionized.[8,15,17,22,23] The probability for CIN (and re-ionization) depends strongly on the ion-target combination, because the ground-state promotion depends on the energy of the ground state relative to the core levels of the target atom.[20,21] The neutralization probability furthermore depends on the velocity of the ion, which determines the time available for resonant charge transfer to the ground state.

In this paper we argue that CIN is an important neutralization mechanism for noble gas ions scattered from alkali and alkali-earth elements. Moreover, at high work functions it is the dominant neutralization mechanism for these elements.

### C. Resonant neutralization

Neutralization of noble gas ions is also possible by resonant electron transfer to the first excited level of the ion. This mechanism is similar to neutralization for alkali ions,[24,25] where the energy of the ground state is comparable to the first excited level of noble gas ions. Although several studies have suggested the possibility for this mechanism,[2,4,8] here we show it does indeed take place, but only at low work functions. Moreover, at work functions of the order of 2 eV, RN may become the dominant mechanism for noble gas ions.

The RN can be described as follows. When an ion is near the surface, the population of the shifted and broadened level is in equilibrium with the substrate and will become occupied up to the Fermi edge (see Fig. 1). Along the outgoing trajectory, the charge exchange rate decreases with increasing distance and becomes small compared to the rate of level shifting and narrowing. At a distance referred to as the freezing distance the equilibrium is ''frozen'' (approximately of 2–4 Å), and the extent to which the level is filled at this distance determines the charge fraction.[26,27] With increasing velocity of the ions, the freezing distance decreases, and consequently the neutralization probability decreases. Furthermore, from Fig. 1 it is also apparent that the neutralization probability is determined by the position of the Fermi edge and thus depends on the work function.

Due to RN, the noble gas ions are in an excited state as they leave the surface. Deexcitation of the excited noble gas ion cannot take place by a direct transition of the electron to the ground state under the emission of a photon [according to Hund's rules this is a forbidden transition with $\Delta l=0$ $(2s \rightarrow 1s)$]. Therefore, deexcitation has to occur through Auger deexcitation or autodetachment.[28–32] The transition rates of these deexcitation processes are approximately one order of magnitude smaller than the transition rates for resonant charge exchange.[28,33] Therefore, it is expected that RN to the first excited level can in first order be treated without taking deexcitation into account.

### D. Neutralization probability

Despite the fundamental differences between these neutralization mechanisms, the neutralization probability for

each mechanism has a similar dependence on the velocity of the ion. The probability that the incident ion leaves the surface as an ion after interaction(s) with the surface atom(s) is represented by the ion fraction $P^+$, which depends on the ion velocity $v$ according to[14,25,34]

$$P^+ = \exp\,[-v_c(1/v)]. \tag{1}$$

The characteristic velocity $v_c$ is a measure for the neutralization rate, where the physical parameters that determine the characteristic velocity depend on the type of mechanism. The exact definition of the reciprocal ion velocity $1/v$ depends on the neutralization mechanism and whether the interaction involves only the direct scattering partner or more neighboring surface atoms. AN takes place at a distance of approximately 1–2 Å from the scattering partner and can involve neighboring atoms on the incoming and outgoing trajectories. Therefore, the reciprocal ion velocity is defined as $1/v = 1/v_i^\perp + 1/v_f^\perp$, where $v_i^\perp$ and $v_f^\perp$ are the velocities of the ion normal to the surface on the incoming and outgoing trajectories, respectively (Hagstrum model).[13,14] CIN involves only the direct scattering partner, and the velocities relative to the target atom are used, defining the reciprocal ion velocity as $1/v = 1/v_i + 1/v_f$ (as in the Godfrey-Woodruff model).[10,35,36] For RN involving the first excited level, the neutralization probability is determined at distances of 2–4 Å, and thus like the Auger process the interaction involves more than one surface atom.[25] Because the neutralization is determined here on the outgoing trajectory, the reciprocal ion velocity is defined as $1/v = 1/v_f^\perp$. These different definitions of the reciprocal ion velocity imply that the correct choice can only be made once the nature of the mechanism is known. However, independent of this choice, the neutralization behavior can be described by Eq. (1), and only the magnitude of the characteristic velocity is influenced by the choice of $1/v$. It should thus be stressed that even when it is not known which mechanism is dominant, independent of the choice of the definition of the reciprocal velocity, the experimental results still obey Eq. (1) for the mechanisms discussed above. This is also true if more than one mechanism contributes to the neutralization. The value of the characteristic velocity that we obtain by fitting the experimental results will, however, depend on the choice of our definition.

Here we have not discussed the quasiresonant core-level neutralization that takes place for some ion-target combinations, like, e.g., $He^+$-Pb,[34,37] since it is a rather exceptional process that yields an oscillatory neutralization behavior as a function of the velocity.

## III. EXPERIMENT

### A. Setup

The investigations were performed in the UHV setup MiniMobis, which has a base pressure of $1\times10^{-10}$ mbar and is described elsewhere.[5,38] Instrumentation was available for LEIS, Auger electron spectroscopy (AES), and low-energy electron diffraction (LEED). The ion scattering was performed using $He^+$, $Ne^+$, and $Ar^+$ noble gas ions with an initial energy between 2 and 5 keV. The incident ion beam was directed perpendicular to the surface, and the ions that scattered back over an angle of 136° were analyzed by a cylindrical mirror analyzer (CMA). Auger electron spectroscopy was performed with the use of a grazing incidence electron beam, where electrons were directed towards the sample at an angle of 10° with the surface plane. The Auger electrons were detected by the same CMA as used for the ion scattering. The work functions of the surfaces were derived from the onset of the secondary electron emission,[39–41] where the secondary electrons were created by the AES electron beam. Since this method is a relative work function measurement technique, a clean W(110) substrate was used as a reference [$\varphi = 5.4$ eV (Ref. 42)]. The characterization and cleaning procedures of the W substrate have been reported elsewhere.[43]

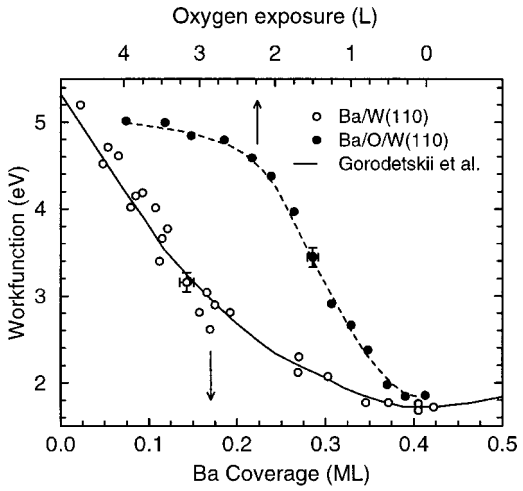


FIG. 2. Work function of the Ba/W(110) system vs the Ba coverage (open circles). The solid line represents the results of Gorodetskii and Melnik (Ref. 47). The work function of the Ba/O/W(110) system is shown vs the oxygen exposure (solid circles). For clarity only one error bar is shown per curve to indicate the uncertainty in the data points: the uncertainty for the other points on the curve are the same as for the point indicated.

### B. Methods of inducing the work function change

We adsorbed submonolayers of Ba atoms on W(110) and Re(0001) single crystals in order to investigate the neutralization over a large work function range. The work function change induced by Ba adsorption is similar to the behavior observed in alkali-metal systems:[44–46] at each adsorption site the charge donation to the substrate leads to the creation of a dipole antiparallel to the surface dipole, thereby causing a decrease of the work function. Figure 2 shows the work function of the Ba/W(110) system as a function of Ba coverage (open circles). The Ba coverage was deduced from the Ba(512 eV)/W(169 eV) Auger signal ratio and calibrated by assigning the work function minimum of $\varphi = 1.8$ eV to a coverage of $\theta_{Ba} = 0.4$ ML.[42] One monolayer corresponds to a Ba density of $6.3\times10^{14}$ atoms/cm$^2$ for a close-packed hexagonal structure. The accuracy of the coverage and work function measurements is indicated by the error bars in Fig. 2; for each curve, we show only one error bar for clarity, but

the other points of the same curve have the same error bars. The solid curve represents the results from Gorodetskii and Melnik for the work function of the Ba/W(110) system.[47] The work function curve for the Ba/Re(0001) system is not presented, but shows a similar dependence on the Ba coverage.[48] The electrostatic repulsion between the different Ba dipoles results in a uniform distribution of the Ba atoms across the substrate for both the Ba/W and the Ba/Re system.[47]

As an alternative method of inducing work function changes, the Ba/W(110) system at a fixed Ba coverage of $\theta_{Ba}=0.4$ ML ($\varphi=1.8$ eV) was exposed to an increasing amount of oxygen (0–4 L). The oxygen adsorption leads to depolarization of the Ba-W dipoles and counteracts the effect of the alkali-earth adsorption.[49–51] The oxygen exposure thus increased the work function to a value that is close to that of clean W(110). Figure 2 also shows the work function for the Ba/O/W(110) system as a function of oxygen exposure (solid circles).

### C. Characteristic velocity method

The characteristic velocity can be derived from the dependence of the measured LEIS signal on the initial energy of the ions. The LEIS signal $S_k(E_i)$ for ions with initial energy $E_i$ scattering from species $k$ is defined as the area of the corresponding peak in the LEIS spectrum and is proportional to the surface density $n_k$ and the ion fraction $P_k^+(E_i)$ (Ref. 38):

$$S_k(E_i)=\varepsilon(E_i)T(E_i)\frac{d\sigma_k}{d\Omega}(E_i)P_k^+(E_i)n_k. \qquad (2)$$

Here $\varepsilon(E_i)$ and $T(E_i)$ are the ion detection efficiency and the analyzer transmission, respectively, which both depend on the energy of the ions.[38,52] The differential scattering cross section $d\sigma_k/d\Omega(E_i)$ depends on the initial ion energy and can be calculated by using, e.g., the Molière approximation to the Thomas-Fermi potential.[53,54] The influence of the roughness on the LEIS signal is neglected here because well-ordered flat single crystals are used. Combining Eqs. (1) and (2), we find

$$\ln\left(\frac{S_k(E_i)}{\varepsilon(E_i)T(E_i)\dfrac{\partial\sigma_k}{\partial\Omega}(E_i)}\right)=\ln(n_k)-v_c^k\frac{1}{v}(E_i). \qquad (3)$$

This equation shows that the characteristic velocity $v_c^k$ for scattering from species $k$ can be derived from the energy dependence of the LEIS signal after correcting for the energy dependences of the detection efficiency, analyzer transmission, and scattering cross section. Plotting the logarithm of the corrected signal versus the reciprocal ion velocity yields the characteristic velocity as the slope of the line. Note that Eq. (3) only holds if the neutralization mechanisms remain the same over the energy range being studied. If a neutralization mechanism is only operating in part of the energy range or the characteristic velocity for a process changes, the plot will not show a simple straight line and the analysis does not work.

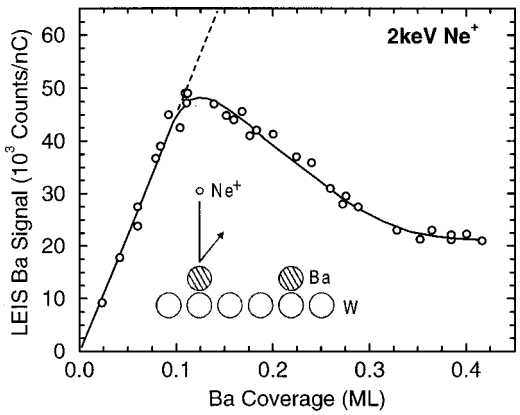


FIG. 3. LEIS signal of 2-keV $Ne^+$ ions scattered from the Ba adatoms as a function of Ba coverage. The dashed line represent the extrapolation of linear behavior observed at low coverages.

At infinite velocity the ion fraction equals unity, and thus the surface density $n_k$ of the species under investigation can be derived by extrapolating the LEIS signal to infinite velocity. It should be noted that in general caution is required in such an extrapolation, since it is only valid if the neutralization mechanism follows Eq. (1) with a constant characteristic velocity over the entire energy range: we refer to the literature for details on using the extrapolation method for this system.[55]

If the instrumental energy dependences of the setup are not exactly known, the characteristic velocity cannot be correctly derived. For our LEIS setup the energy dependences of the detection efficiency and analyzer transmission have been investigated and reported elsewhere.[38]

## IV. RESULTS AND DISCUSSION

### A. Evidence for work function dependent neutralization

A demonstration of the influence of the work function on the neutralization of the ions is given in Fig. 3. Here the ion scattering signal for 2-keV $Ne^+$ ions scattered from Ba atoms is shown as a function of Ba coverage. For low Ba coverages ($\theta_{Ba}<0.12$ ML) and corresponding high work functions ($\varphi>3.4$ eV) the Ba signal is proportional to the Ba coverage, as expected for a constant neutralization probability. Above a coverage of $\theta_{Ba}=0.12$ ML a deviation from this proportionality is observed, and the Ba signal decreases with increasing Ba coverage. The W substrate signal continuously decreases with increasing Ba coverage, which indicates that no cluster formation takes place and that the Ba adatoms form a uniform layer.[46,47] Since the initial energy of the $Ne^+$ ions was fixed, the detection efficiency, analyzer transmission, and scattering cross section are constant. The observed behavior can therefore only be explained by a strong continuous decrease of the ion fraction with increasing coverage; the signal decreases because the ion fraction decreases faster than the Ba density increases. Identical trends in the signal intensity versus coverage have been observed for $He^+$, $Ne^+$, and $Ar^+$ ions. Evidently, above a certain Ba coverage—i.e., below a certain work function—an additional neutralization channel is available, and Eq. (3) does not describe the ion

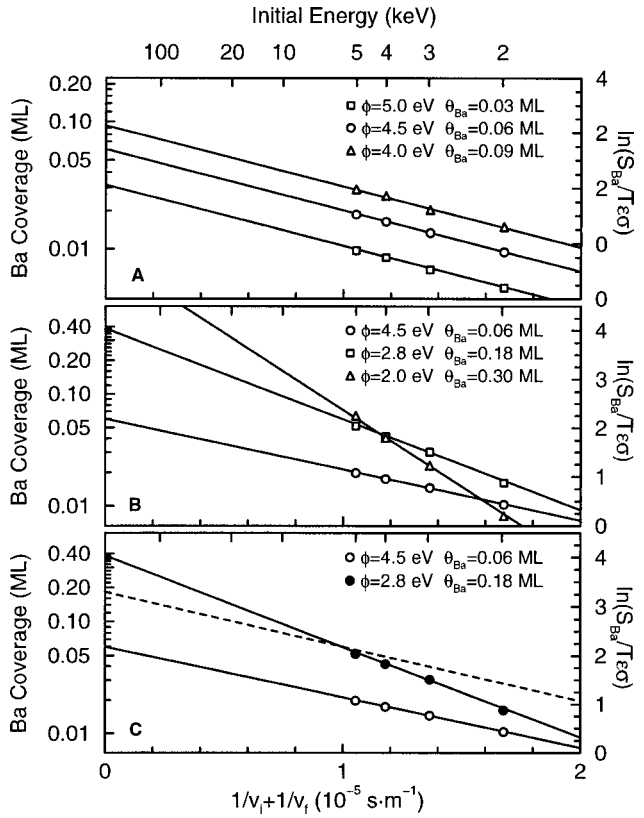


FIG. 4. Characteristic velocity plots for different work functions. The initial energy scale is shown on the top axis. The solid lines show linear regressions to the data, where the slopes represent the characteristic velocities. (a) High work functions, (b) low work functions, and (c) contribution from resonant neutralization. The dashed line is explained in Sec. IV D.

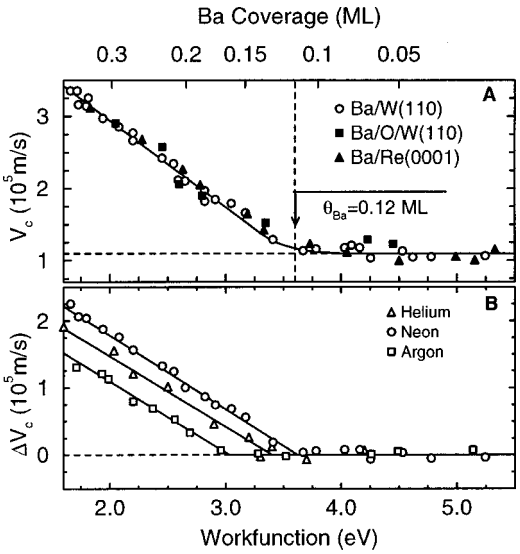


FIG. 5. (a) Characteristic velocities for $Ne^+$ ions scattered from the Ba adatoms as a function of the work function. The open circles correspond to Ba adsorption on W(110), the solid squares to Ba and O coadsorbed on the W(110) surface, and the solid triangles to Ba adsorbed on the Re(0001) surface. The vertical dashed line represents the onset of the low-work-function mechanism. (b) The increase in the characteristic velocity for the different ions relative to the characteristic velocity at high work functions.

scattering yield correctly with the same characteristic velocity for different work functions.

### B. Characteristic velocity versus work function

In Fig. 4 several characteristic velocity plots for $Ne^+$ ions scattered from Ba adatoms are presented to demonstrate the influence of the work function on the neutralization behavior. Here the Ba signal corrected for the instrumental energy dependence (right ordinate scale) is shown versus the reciprocal velocity. Extrapolation of the data points to infinite velocity yields the Ba coverage on the left ordinate scale. The reciprocal velocity was calculated as $1/v = 1/v_i + 1/v_f$ based on the CIN mechanism, as explained in Sec. II D.

In Fig. 4(a) (top panel) the characteristic velocity plots are shown for $\varphi > 3.4$ eV, where the Ba signal is proportional to the Ba coverage. For these high work functions the characteristic velocity, represented by the slope of the line, is constant. This indicates that at high work functions the noble gas ions are neutralized by a mechanism insensitive to work function changes. In addition, it is observed that the extrapolation to infinite velocity gives the correct Ba coverage as calibrated by Auger analysis.

In Fig. 4(b) (middle panel) the characteristic velocity plots are shown for $\varphi < 3.4$ eV, where the Ba signal decreases with increasing Ba coverage. For comparison, the characteristic velocity plot for a work function of $\varphi = 4.5$ eV is also shown. The characteristic velocity clearly increases with decreasing work function. Thus at low work functions a mechanism occurs where the neutralization probability depends on the work function. Furthermore, it is apparent that the extrapolation to infinite velocity results in an overestimation of the Ba coverage. The explanation for this overestimation is given in Sec. IV D.

The characteristic velocities derived from these plots are shown in Fig. 5(a) versus the work function. The figure shows a constant characteristic velocity plateau at high work functions ($\varphi > 3.4$ eV) and a linear increase of the characteristic velocity at low work functions ($\varphi < 3.4$ eV). Identical trends in the characteristic velocity versus work function curve are observed for $He^+$, $Ne^+$, and $Ar^+$ ions: only the threshold below which the low-work-function neutralization channel is available depends on the ion type (see Table I). The characteristic velocity values of the high-work-function plateau also depend on the ion type and are summarized in Table I. Figure 5(b) shows the increase in the characteristic velocity relative to the constant value observed at high work functions. For example, the $Ne^+$ curve in Fig. 5(b) is obtained by subtracting a value of $v_c = 1.12 \times 10^5$ m/s from the entire characteristic velocity curve in Fig. 5(a).

### C. Auger versus collision-induced neutralization

In this section we discuss the basic neutralization mechanism for noble gas ions that is available at all work functions. Resonant neutralization involving the first excited level can only take place at low work functions and is there-

TABLE I. Overview of the neutralizaton results for the different ions scattered from Ba and W atoms. $E_g$ = energy of the ground state. $E_i$ = energy of the first excited level. $\phi_{\text{onset}}$ = work function threshold for low-work-function mechanism. $v_c$(Ba) = characteristic velocity for Ba at $\theta_{\text{Ba}} = 0$ ML. $V_c(W)$ = characteristic velocity for W at $\theta_{\text{Ba}} = 0$ ML.

| | $E_g$ (eV) | $E_i$ (eV) | $\phi_{\text{threshold}}$ (eV) | $v_c$ (Ba) ($10^5$ m s$^{-1}$) | $v_c$ (W) ($10^5$ m s$^{-1}$) |
|---|---|---|---|---|---|
| $He^+$ | 24.6 | 4.77 | $3.2 \pm 0.05$ | $4.72 \pm 0.15$ | $3.20 \pm 0.15$ |
| $Ne^+$ | 21.6 | 4.95 | $3.4 \pm 0.05$ | $1.12 \pm 0.11$ | $1.70 \pm 0.08$ |
| $Ar^+$ | 15.8 | 4.21 | $2.9 \pm 0.05$ | $0.72 \pm 0.08$ | $1.81 \pm 0.10$ |

fore not considered here (see Sec. IV D). Neutralization can thus take place by either AN or CIN. We focus on the results for $He^+$ ions since most of the neutralization studies in the literature use $He^+$ ions. Figure 6 presents the characteristic velocities for $He^+$ scattered from various targets throughout the periodic system as determined by Mikhailov *et al.*[18] using an initial energy range between 1 and 3.5 keV (open symbols). The characteristic velocities determined in this work for $He^+$ scattered from Ba and W atoms in the high-work-function limit ($\varphi > 3.4$ eV) are indicated by crosses ($\times$). Figure 6 also shows the re-ionization probabilities for $He^+$ ions for various target atoms as determined by Souda *et al.*[17] (solid symbols). The striking similarity between the re-ionization and neutralization trends across the periodic system was already noted by Mikailov *et al.* and strongly suggests that CIN plays an important role in the neutralization of noble gas ions (see Sec. II).

The characteristic velocities determined here for Ba and W fit very well in the observed trends. These trends in the re-ionization have been qualitatively explained by Tsukada *et al.*,[20,21] who calculated the level promotion of the ground state during the close encounter of $He^+$ ions and various target atoms. These calculations show that for the VIII-$II_b$ elements no or little promotion takes place, while for the elements in the first columns of the periodic system the ground state of the noble gas ions is strongly promoted. Thus the minimum in the characteristic velocities in Fig. 6 around the VIII-$II_b$ elements is caused by the absence of sufficient promotion and the resulting absence of CIN.

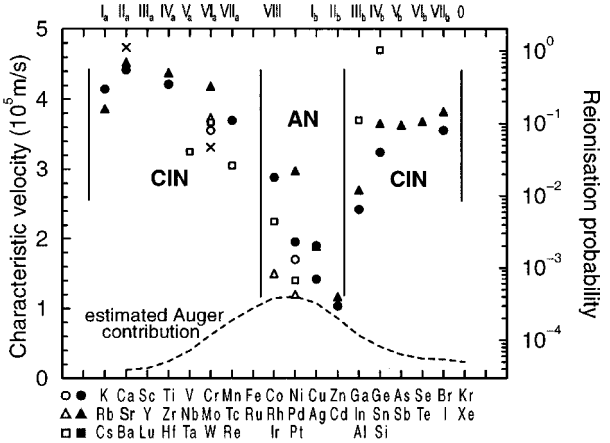


FIG. 6. Characteristic velocities for $He^+$ ions scattered from various elements in the periodic table as measured by Mikhailov *et al.* (Ref. 18) (open symbols). For comparison, the re-ionization probabilities as measured by Souda *et al.* (Ref. 17) are also shown (solid symbols). The characteristic velocities for $He^+$ scattered from Ba and W are indicated by the crosses ($\times$). The dashed line represents the estimated Auger contribution based on the electron density and assuming a dominant Auger neutralization for Pd.

Goldberg *et al.*[19] performed *ab initio* calculations of the neutralization of $He^+$ ions scattered from Pd and concluded that in this case CIN is not significant, but that AN is dominant. Assuming that the characteristic velocity for Pd in Fig. 6 is completely due to AN, we can estimate the upper limit of the Auger contributions across the periodic system. The AN rate is in first-order approximation proportional to the square of the density of electrons available for the transition (see Sec. II). The estimated Auger contribution is indicated in Fig. 6 by the dashed curve, where the electron density for the various elements was calculated by dividing the number of valence electrons by the atomic volume.

We conclude that for neutralization of $He^+$ ions scattered from Ba adatoms and all alkali and alkali-earth elements, the Auger mechanism plays no significant role. The neutralization thus must be dominated by CIN at high work functions. We emphasize that this conclusion is only valid for the initial energies used here. At lower energies ($<0.5$ keV), CIN will often not be possible due to the threshold energy for sufficient promotion, and consequently the neutralization will be dominated by AN. Furthermore, the conclusion is also only valid for the small impact parameters that are required for the ions to be backscattered (impact parameters in this study range between 0.02 and 0.09 Å). At large impact parameters the ground level promotion is not sufficient for CIN to take place, and AN will be the dominant mechanism. To determine at which impact parameter and energy AN becomes important needs further experimental and theoretical work.

That CIN is the dominant neutralization mechanism is in agreement with the observed insensitivity of the characteristic velocity to the work function (at high work functions). The ground-state promotion of the ions is determined by the core levels of the target, and the resulting resonant charge transfer involves the levels at the bottom of the conduction band. The neutralization probability due to CIN is therefore not expected to be sensitive to work function changes. Although Fig. 5 shows that the characteristic velocity increases at low work functions, CIN is expected to be work function independent over the whole work function range. The contribution of CIN is indicated in the figure by the horizontal dashed line. The characteristic velocity due to RN at low

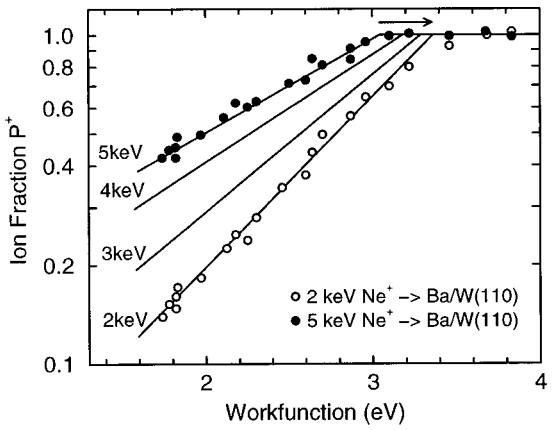


FIG. 7. Ion fraction exclusively due to the resonant neutralization mechanism. Note the logarithmic scale of the ion fraction. Only the 2- and 5-keV data points are shown for clarity. The arrow indicates the difference in onset of the low-work-function mechanism.

work functions (see Sec. IV D) is superimposed on the characteristic velocity due to CIN.

A similar neutralization behavior is observed for $He^+$, $Ne^+$, and $Ar^+$ ions [see Fig. 5(b)], which suggests that CIN is also the dominant mechanism for $Ne^+$ and $Ar^+$ ions at high work functions. However, definite conclusions can only be made when more results for neutralization of these ions during scattering from various target atoms across the periodic system become available.

### D. Resonant neutralization at low work functions

In order to show that neutralization of noble gas ions at low work functions takes place by RN to the first excited level, we will demonstrate that the behavior observed in this work can be described by resonant charge exchange theory. We start by extracting that part of the neutralization probability that is exclusively due to RN at low work functions. The approach is demonstrated in Fig. 3 for $Ne^+$ ions. The proportionality between signal and coverage observed for $\theta_{Ba} < 0.12$ ML is extrapolated to larger coverages as is indicated by the dashed line. The extrapolation is only shown up to $\theta_{Ba}=0.15$ ML, but actually extends to a signal intensity of $1.8\times10^5$ counts/nC for a coverage of $\theta_{Ba}=0.4$ ML. This line thus represents the hypothetical ion scattering signal in case CIN and AN were the only available mechanisms and RN were absent. The decrease of the measured signal compared to the dashed line is thus ascribed to RN. The ion fraction due to this mechanism is obtained by dividing the measured signal intensity (solid curve in Fig. 3) by the hypothetical signal intensity (dashed line in Fig. 3). The resulting ion fractions for $Ne^+$ scattered from Ba are shown in Fig. 7 on a logarithmic scale versus the work function for different initial energies. It is observed that the ion fraction decreases exponentially with decreasing work function, where the rate of decrease diminishes with increasing initial energy. Moreover, the work function below which RN is possible depends on the initial energy of the ions.

These observations can be explained as follows. When the work function decreases, the Fermi level is raised and the fraction of the broadened first excited level that is filled at the freezing distance increases (see Fig. 1). Therefore, the neutralization probability increases with decreasing work function. Resonant charge exchange theory predicts for the ion fraction[27,56]

$$P^+ = \exp\left(-C\frac{\varepsilon_a - \varepsilon_F}{\gamma v}\right). \tag{4}$$

Here $\varepsilon_a$ is the energy of the first excited state at the freezing distance and $\varepsilon_F$ is the Fermi level of the metal (see Fig. 1). The constant $C$ depends on the details of the charge exchange model used,[24,59] but its value is not relevant for the discussion here. The velocity is defined as $v=v_f^{\perp}$ because the neutralization probability is determined on the outgoing trajectory. The decay constant $\gamma$ describes the decrease of the width $\Delta(z)$ of the first excited level with increasing distance $z$ between the ion and surface:

$$\Delta(z) = \Delta_0 e^{-\gamma z}. \tag{5}$$

The exponential decrease of the ion fraction with decreasing work function as observed in Fig. 7 is thus consistent with the theory. Moreover, Eq. (4) predicts that the characteristic velocity increases linearly with decreasing work function, as observed from Fig. 5. The increase of the characteristic velocity with decreasing work function is similar for the different ions [see Fig. 5(b)], which suggests that the decay constants $\gamma$ are comparable for the ions. Although to our knowledge no reports are available in the literature that compare the decay constants for different noble gas ions,[57] this similarity is reasonable since calculations of the level widths show the decay constants to be comparable for different alkali ions.[58]

Resonant neutralization to the first excited level is not possible when the Fermi level is equal to the energy of the excited level for the ion at rest at infinite distance from the surface (see Fig. 1). This is consistent with Fig. 5, where the work function below which RN is possible is approximately 1.5 eV lower than expected based on the energy of the level at infinite distance from the surface (see Table I). This lower work function compared to the energy of the first excited level is caused by the level shift of the ions near the surface.[56,59,60] The shift of the first excited level a few angstrom from the surface where the charge state is frozen is of the order of 1 or 2 eV.[13,14] For RN to take place, the Fermi level has to be near or above the energy of the first excited level at the freezing distance. Hence the energy $\varepsilon_a$ is defined at the freezing distance. For example, if in Fig. 1 the Fermi edge is aligned with the energy of the first excited level for the ion at infinite distance from the surface (dashed line in Fig. 1), no neutralization is possible. The difference between the energy of the first excited level and the work function threshold for RN is similar for the different ions because the level shifts of the ions are comparable at the freezing distance.[13,14]

The dependence of the work function threshold on the energy of the ions, as seen in Fig. 7, occurs because the freezing distance decreases with increasing velocity.[24,25] When the freezing distance decreases, the energy $\varepsilon_a$ in-

creases, and thus the work function below which RN can take place decreases. Note that in neutralization of alkali ions no clear dependence of the work function threshold for RN on the energy of the ions is observed at energies well below 1 keV, because the level shift changes very little with distance at large freezing distances. Since the work function below which RN occurs depends on the ion energy, the relative importance of CIN and RN depends on the ion energy for a fixed work function. This is demonstrated in Fig. 4(c), where a characteristic velocity plot is shown for a work function $\varphi = 2.8$ eV (solid circles). For comparison, the characteristic velocity plot for $\varphi = 4.5$ eV, where only CIN is possible, is also shown (open circles). The dashed line corresponds to the hypothetical neutralization behavior at $\varphi = 2.8$ eV in the absence of RN. The decrease of the measured signal compared to the dashed line is caused by RN. As expected from Fig. 7, at a work function of $\varphi = 2.8$ eV, RN has a very small influence for an initial energy of 5 keV, but does lead to a significant signal decrease for lower initial energies. Because the relative importance of the mechanisms depends on the initial energy, the characteristic velocity method cannot be used to derive the coverage from extrapolation to infinite velocity. Figure 4(c) shows that the extrapolation leads to an overestimation of the derived Ba coverage. Note that the extrapolation of the dashed line in Fig. 4(c) indicates the correct coverage since here only one mechanism is available: collision-induced neutralization. The implications of these observations for a quantitative compositional surface analysis using LEIS at low-work function systems is discussed elsewhere.[55]

We conclude that at low work functions noble gas ions can be neutralized by a resonant electron transfer to the first excited level of the ion. All observations can be described by the resonant charge exchange theory for neutralization of low-energy alkali ions.

### E. Macroscopic work function versus local potential

Investigations of RN of low-energy alkali ions have shown that the neutralization probability is governed by the macroscopic work function.[56,58,61] A freezing distance of the order of a few angstrom is in agreement with the concept of a macroscopic work function, since at this distance the local potential of the atoms is smeared out and the electron distribution is rather smooth. However, most of these studies have used initial ion energies well below 1 keV. To validate whether the concept of a macroscopic work function can be extrapolated to higher initial energies and corresponding smaller freezing distances, the method of inducing the work function changes was varied. A comparison of the neutralization behavior of the Ba/W, Ba/Re, and Ba/O/W systems is performed in Fig. 5(a), where the characteristic velocities for $Ne^+$ ions scattered from Ba adatoms are shown versus the work function (see also Sec. III B). Note that the oxygen in the Ba/O/W system is positioned in the plane between the Ba and W atoms and does not shield the Ba atoms from the incident ions.[2,62]

For these different systems, the characteristic velocity shows the same dependence on work function, independent of the method of inducing the work function changes. However, the local potentials of the Ba atoms at a certain work function are not identical. The work function decrease for the Ba/W system is achieved by increasing the number of Ba-W dipoles, where the dipole strength remains approximately constant up to a coverage of $\theta_{Ba} = 0.3$ ML. In contrast, for the Ba/O/W system the density of the dipoles equals the Ba density at the work function minimum, but due to the adsorption of oxygen, the average dipole strength decreases and the work function increases. Therefore, for the same macroscopic work function, both systems have different local potentials of the Ba atoms. Similarly, because the work function of the clean Re(0001) substrate is larger than for the clean W(110) substrate ($\varphi_{Re} = 6.0$ eV), an identical macroscopic work function for the Ba/W and Ba/Re systems requires a different dipole arrangement. We can thus conclude that also for noble gas ions at initial energies of a few keV, the neutralization probability of the resonant mechanism is governed by the macroscopic work function.

## V. CONCLUSIONS

We have investigated the neutralization of noble gas ions by studying the neutralization probability of $He^+$, $Ne^+$, and $Ar^+$ ions scattered from Ba atoms on surfaces with different work functions. Through combining our results with those of previous neutralization studies available in the literature, we have shown that for noble gas ions scattered from Ba atoms and other alkali(-earth) elements, collision-induced neutralization is the dominant process. It should be stressed that this is only valid for the initial energies (2–5 keV) and small impact parameters (typically up to 0.09 Å) used here. At lower energies or larger impact parameters CIN might not be possible because the ground state is insufficiently promoted, and then the neutralization will be dominated by AN. The neutralization probability due to CIN is insensitive to work function changes since the promotion depends on the core levels of the target atoms. Moreover, since CIN takes place during the close encounter between the ion and target atom, the neutralization probability is expected to be insensitive to the scattering geometry.

Resonant neutralization to the first excited level of the noble gas ions was observed at low work functions. The work function dependence of the neutralization probability is consistent with the resonant charge exchange theory. Resonant neutralization is only possible below a certain work function, which depends on the ionization potential of the first excited level and on the velocity of the ion. The neutralization probability due to the resonant mechanism increases exponentially with decreasing work function, while the rate of increase is determined by the velocity of the ion and the decay constant of the level width. In contrast to AN and CIN, the neutralization probability for this resonant channel is not determined by the specific ion-target combination, but rather is governed by the macroscopic work function. Consequently, the neutralization probability is determined by the velocity of the ion perpendicular to the surface and thus depends not only on the energy of the ion, but also on the scattering geometry.

**ACKNOWLEDGMENTS**

We would like to thank Georg Gärtner from Philips Forschungslaboratorien (Aachen, Germany) and Albert Manenschijn from Philips Components (Eindhoven, Netherlands) for discussions and financial support of this work as a part of a collaboration to study the surface of low-work-function thermionic dispenser cathodes by low-energy ion scattering.[5] We also acknowledge support by the Organization for the Advancement of Scientific Research in the Netherlands (NWO).

*Corresponding author. FAX: +31 40 2453587. Electronic address: H.H.Brongersma@tue.nl

[1] H. H. Brongersma and W. J. Schouten, Acta Electron. **18**, 47 (1975).
[2] C. R. K. Marrian, A. Shih, and G. A. Haas, Appl. Surf. Sci. **24**, 372 (1985).
[3] M. J. Ashwin and D. P. Woodruff, Surf. Sci. **244**, 247 (1991).
[4] M. Beckschulte and E. Taglauer, Nucl. Instrum. Methods Phys. Res. B **78**, 29 (1993).
[5] A. W. Denier van der Gon, M. F. F. K. Jongen, H. H. Brongersma, U. van Slooten, and A. Manenschijn, Appl. Surf. Sci. **111**, 64 (1997).
[6] R. Cortenraad, A. W. Denier van der Gon, H. H. Brongersma, G. Gaertner, and A. Manenschijn, Appl. Surf. Sci. **146**, 69 (1999).
[7] F. W. Meyer, L. Folkerts, I. G. Hughes, S. H. Overbury, D. M. Zehner, P. A. Zeijlmans van Emmichoven, and J. Burgdörfer, Phys. Rev. A **48**, 4479 (1993).
[8] R. Souda and M. Aono, Nucl. Instrum. Methods Phys. Res. B **15**, 114 (1986).
[9] R. J. MacDonald and P. J. Matin, Surf. Sci. **111**, L739 (1981).
[10] G. Verbist, J. T. Devreese, and H. H. Brongersma, Surf. Sci. **233**, 323 (1990).
[11] L. K. Verhey, B. Poelsema, and A. L. Boers, Nucl. Instrum. Methods **132**, 565 (1976).
[12] A. L. Boers, Nucl. Instrum. Methods Phys. Res. B **4**, 98 (1984).
[13] H. D. Hagstrum, Phys. Rev. **96**, 336 (1954).
[14] H. D. Hagstrum, in *Inelastic Ion-Surface Collisions*, edited by H. H. Tolk and J. C. Tully (Academic, New York, 1977), p. 1.
[15] M. Aono and R. Souda, Nucl. Instrum. Methods Phys. Res. B **27**, 55 (1987).
[16] W. More, J. Merino, R. Monreal, P. Pou, and F. Flores, Phys. Rev. B **58**, 7385 (1998).
[17] R. Souda, T. Aizawa, C. Oshima, and Y. Ishizawa, Nucl. Instrum. Methods Phys. Res. B **45**, 364 (1990).
[18] S. N. Mikhailov, R. J. M. Elfrink, J.-P. Jacobs, L. C. A. van den Oetelaar, P. J. Scanlon, and H. H. Brongersma, Nucl. Instrum. Methods Phys. Res. B **93**, 148 (1994).
[19] E. C. Goldberg, R. Monreal, F. Flores, H. H. Brongersma, and P. Bauer, Surf. Sci. **440**, L875 (1999).
[20] M. Tsukada, S. Tsuneyuki, and N. Shima, Surf. Sci. **164**, L811 (1985).
[21] S. Tsuneyuki and M. Tsukada, Phys. Rev. B **34**, 5758 (1986).
[22] R. Souda, T. Aizawa, C. Oshima, S. Otani, and Y. Ishizawa, Phys. Rev. B **41**, 803 (1990).
[23] T. M. Thomas, H. Neumann, and A. W. Czanderna, Surf. Sci. **175**, L737 (1986).
[24] R. Brako and D. M. Newns, Rep. Prog. Phys. **52**, 655 (1989).
[25] J. Los and J. J. C. Geerlings, Phys. Rep. **190**, 134 (1990).
[26] E. G. Overbosch, B. Rasse, A. D. Tenner, and J. Los, Surf. Sci. **92**, 310 (1980).
[27] J. K. Norskov and B. L. Lundqvist, Phys. Rev. B **19**, 5661 (1979).
[28] R. J. A. van den Oetelaar and C. F. J. Flipse, Phys. Rev. B **52**, 10 807 (1995).
[29] H. D. Hagstrum, P. Petrie, and E. E. Chaban, Phys. Rev. B **38**, 10 264 (1988).
[30] R. Souda, W. Hayami, T. Aizawa, S. Otani, and Y. Ishizawa, Phys. Rev. B **46**, 7315 (1992).
[31] H. Mueller, R. Hausmann, H. Brenten, A. Niehaus, and V. Kempter, Z. Phys. D: At., Mol. Clusters **28**, 109 (1993).
[32] F. Wiegershaus, S. Krischok, D. Ochs, W. Maus-Friedrichs, and V. Kempter, Surf. Sci. **345**, 91 (1996).
[33] W. Sesselmann, B. Woratschek, J. Kueppers, and G. Ertl, Phys. Rev. B **35**, 1547 (1987).
[34] D. P. Woodruff, Nucl. Instrum. Methods Phys. Res. **194**, 639 (1982).
[35] D. J. Godfrey and D. P. Woodruff, Surf. Sci. **105**, 438 (1981).
[36] D. J. Godfrey and D. P. Woodruff, Surf. Sci. **105**, 459 (1981).
[37] W. Bloss and D. Hone, Surf. Sci. **72**, 277 (1978).
[38] R. Cortenraad, A. W. Denier van der Gon, and H. H. Brongersma, Surf. Interface Anal. **29**, 524 (2000).
[39] A. P. Janssen, P. Akhter, C. J. Harland, and J. A. Venables, Surf. Sci. **93**, 453 (1980).
[40] G. Eng and H. K. A. Kan, Appl. Surf. Sci. **8**, 81 (1981).
[41] H. Oechsner, Fresenius J. Anal. Chem. **355**, 419 (1996).
[42] In *Gmelin Handbook of Inorganic and Organometallic Chemistry*, edited by E. Koch and W. Huisl, Tungsten Supplement Vol. A 6a (Springer-Verlag, Berlin, 1991).
[43] S. N. Ermolov, R. Cortenraad, V. N. Semenov, A. W. Denier van der Gon, S. I. Bozhko, H. H. Brongersma, and V. G. Glebovsky, Vacuum **53**, 83 (1999).
[44] K. Wandelt, in *Physics and Chemistry of Alkali Metal Adsorption*, edited by H. P. Bonzel, A. M. Bradshaw, and G. Ertl (Elsevier, Amsterdam, 1989), p. 25.
[45] H. Ishida, Phys. Rev. B **38**, 8006 (1988).
[46] E. Wimmer, A. J. Freeman, J. R. Hiskes, and A. M. Karo, Phys. Rev. B **28**, 3074 (1983).
[47] D. A. Gorodetskii and Y. P. Melnik, Surf. Sci. **62**, 647 (1977).
[48] D. A. Gorodetskii and A. N. Knysh, Surf. Sci. **40**, 651 (1973).
[49] L. A. Hemstreet, S. R. Chubb, and W. E. Pickett, Phys. Rev. B **40**, 3592 (1989).
[50] G. A. Haas, A. Shih, and C. R. K. Marrian, Appl. Surf. Sci. **16**, 139 (1983).
[51] B. C. Lamartine, J. v. Czarnecki, and T. W. Haas, Appl. Surf. Sci. **26**, 61 (1986).
[52] T. Asahata, M. Onubu, A. Kondo, R. Shimizu, and H. J. Kang, Jpn. J. Appl. Phys., Part 1 **36**, 7427 (1997).
[53] G. Molière, Z. Naturforsch. A **2**, 133 (1947).
[54] C. A. Severijns, Ph.D. thesis, Eindhoven University of Technology, The Netherlands, 1992.
[55] R. Cortenraad, A. W. Danier van der Gon, H. H. Brongersma, S. N. Ermolov, and V. G. Glebovsky, Surf. Interface Anal. **31**, 200 (2001).

[56] M. L. Yu and N. D. Lang, Nucl. Instrum. Methods Phys. Res. B **14**, 403 (1986).
[57] C. A. Moyer and K. Orvek, Surf. Sci. **114**, 295 (1982).
[58] P. Nordlander and J. C. Tully, Surf. Sci. **211/212**, 207 (1989).
[59] M. L. Yu and N. D. Lang, Phys. Rev. Lett. **50**, 127 (1983).
[60] J. J. C. Geerlings, L. F. Kwakman, and J. Los, Surf. Sci. **184**, 305 (1987).
[61] M. L. Yu, Phys. Rev. B **26**, 4731 (1982).
[62] D. Norman and R. A. Tuck, Phys. Rev. Lett. **58**, 519 (1987).